PREPARED FOR THE U.S. DEPARTMENT OF ENERGY,
UNDER CONTRACT DE-AC02-76CH03073

PPPL-3951
UC-70

PPPL-3951

Simultaneous Microwave Imaging System for Density and Temperature Fluctuation Measurements on TEXTOR

by

H. Park, E. Mazzucato, T. Munsat, C.W. Domier, M. Johnson,
N.C. Luhmann, Jr., J. Wang, Z. Xia, I.G.J. Classen,
A.J.H. Donné, and M.J. van de Pol

May 2004

PPPL
PRINCETON PLASMA
PHYSICS LABORATORY

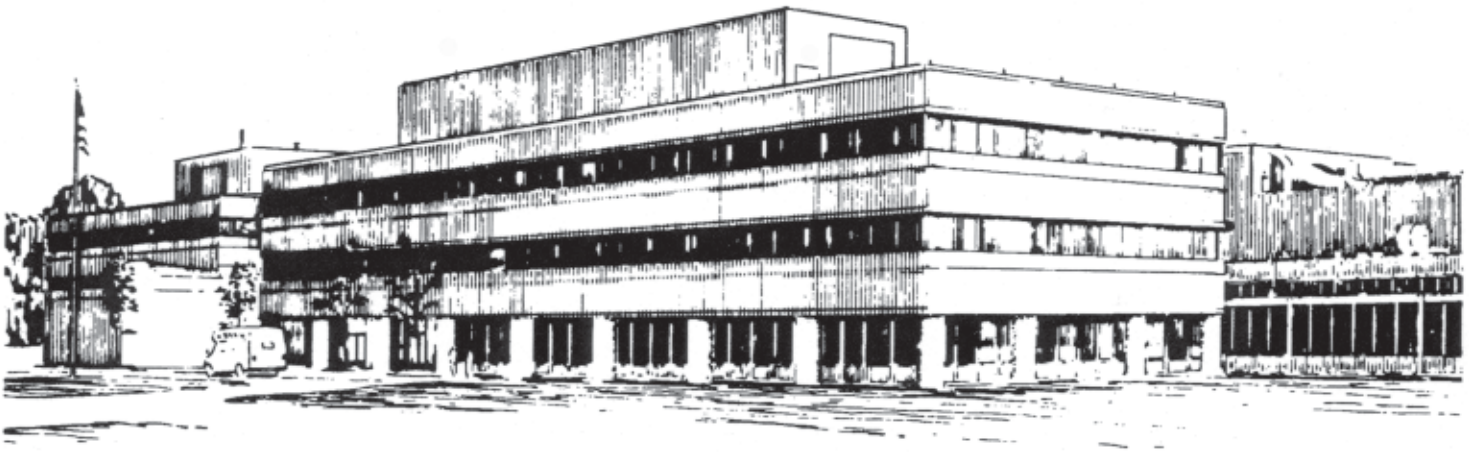

PRINCETON PLASMA PHYSICS LABORATORY
PRINCETON UNIVERSITY, PRINCETON, NEW JERSEY

PPPL Reports Disclaimer

Availability

This report is posted on the U.S. Department of Energy's Princeton Plasma Physics Laboratory Publications and Reports web site in Fiscal Year 2004. The home page for PPPL Reports and Publications is: http://www.pppl.gov/pub_report/

DOE and DOE Contractors can obtain copies of this report from:

U.S. Department of Energy
Office of Scientific and Technical Information
DOE Technical Information Services (DTIS)
P.O. Box 62
Oak Ridge, TN 37831

Telephone: (865) 576-8401

Fax: (865) 576-5728

Email: reports@adonis.osti.gov

This report is available to the general public from:

National Technical Information Service
U.S. Department of Commerce
5285 Port Royal Road
Springfield, VA 22161

Telephone: 1-800-553-6847 or
(703) 605-6000

Fax: (703) 321-8547

Internet: http://www.ntis.gov/ordering.htm

Invited Article: Review of Scientific Instruments, 2004

SIMULTANEOUS MICROWAVE IMAGING SYSTEM FOR DENSITY AND TEMPERATURE FLUCTUATION MEASUREMENTS ON TEXTOR

H. Park, E. Mazzucato, T. Munsat

Plasma Physics Laboratory, Princeton University, Princeton, New Jersey 08543, U.S.A.

C.W. Domier, M. Johnson, N.C. Luhmann, Jr., J. Wang, Z. Xia

Department of Applied Science, University of California at Davis, Davis, California 95616, U.S.A.

I.G.J. Classen, A.J.H. Donné, M.J. van de Pol

FOM-Instituut voor Plasmafysica Rijnhuizen, Associatie EURATOM-FOM, Trilateral Euregio Cluster, 3430 BE, Nieuwegein, The Netherlands

ABSTRACT

Diagnostic systems for fluctuation measurements in plasmas have, of necessity, evolved from simple 1-D systems to multi-dimensional systems due to the complexity of the MHD and turbulence physics of plasmas illustrated by advanced numerical simulations. Using the recent significant advancements in millimeter wave imaging technology, Microwave Imaging Reflectometry (MIR) and Electron Cyclotron Emission Imaging (ECEI), simultaneously measuring density and temperature fluctuations, are developed for TEXTOR. The MIR system was installed on TEXTOR and the first experiment was performed in September, 2003. Subsequent MIR campaigns have yielded poloidally resolved spectra and assessments of poloidal velocity. The new 2-D ECE Imaging system (with a total of 128 channels), installed on TEXTOR in December, 2003, successfully captured a true 2-D images of T_e fluctuations of m=1 oscillation ("sawteeth") near the q~1 surface for the first time.

1. INTRODUCTION

The fluctuations in magnetized plasmas range from small amplitude microturbulence to large amplitude MHD behavior. While microturbulence is of critical importance to basic transport physics, taming of the large MHD fluctuations ultimately responsible for the disruption of current driven toroidal plasmas is also of critical importance for the stability limit of the discharges. Both fluctuations impact the eventual realization of magnetic fusion energy. Recently, significant experimental progress has been made in suppressing micro-turbulence and harmful MHD modes leading to disruptions, thereby simultaneously achieving improved confinement and higher stability limit. Also, the theoretical understanding of plasma turbulence and MHD physics has been greatly enriched with the help of the rapid advancement of computer technology, which, for example, has made it possible in extensive simulations to reveal elegant three-dimensional (3-D) structures of plasma turbulence[1,2] and MHD phenomena[3]. Diagnostic systems for fluctuation measurements in plasmas have, of necessity, evolved from simple 1-D systems to multi-dimensional systems due to the complexity of the turbulence physics of plasmas, as illustrated by advanced numerical simulations. Utilizing the recent significant advancements in millimeter wave imaging technology[4], Microwave Imaging Reflectometry (MIR)[5] and Electron Cyclotron Emission Imaging (ECEI)[6], which simultaneously measure density and temperature fluctuations, have been developed for the study of TEXTOR tokamak plasmas. Extensive testing of the optical system for MIR/ECEI was established with known targets (corrugated metal surfaces) [4,7,8] prior to the installation on TEXTOR. The first MIR test experiment was successfully performed in September, 2003. Subsequent MIR campaigns have yielded poloidally resolved spectra and assessments of the poloidal phase velocity of turbulent structures. In the previous generation ECEI systems[6,9], the measurements were essentially 1-D

in nature in that the detected radiation from each array element was sampled at only a single frequency at a given time, resulting in measurements of vertically distributed plasma volumes. This is in contrast to the conventional wideband ECE radiometer, in which multiple frequency elements are simultaneously detected from a single antenna resulting in a horizontally aligned sampling. The new generation 2-D ECE Imaging system introduced two new technology advances; [1] a dual-dipole antenna array which has significantly improved sensitivity and antenna patterns[10], [2] wideband transmission lines[10], which enable multiple radial measurements for each vertical detection array simultaneously. The new ECEI system with a total of 128 channels, installed on TEXTOR in December, 2003, captured true 2-D image of m=1 mode ("sawteeth" oscillation) near the q~1 ("inversion radius"), for the first time. In this paper, a brief system description of the ECEI/MIR system is given in Sec. 2. Characteristics of the new ECEI system together with the 2D imaging data of m=1 oscillation is provided in Sec. 3. The results of recent experimental campaigns using the MIR system on TEXTOR plasmas are presented in the last section.

2. MIR/ECEI SYSTEM ON TEXTOR

A detailed description of the TEXTOR ECEI/MIR system for can be found in many references[4,5,7,8]. For TEXTOR plasmas, like other tokamaks, the ECE frequency is a monotonically decreasing function of plasma major radius R as $B(R) = B_0 R_0 / R$ as illustrated in Fig. 1, in which the characteristic frequencies are plotted for nominal plasma parameters. Both systems operate in a similar microwave range (the MIR frequency range is ~88 GHz and ECEI ranges from 95 to 130 GHz for TEXTOR). Consequently, it is feasible to combine the two systems which utilize state-of-the-art millimeter-wave planar imaging arrays positioned at the focal point of the detection system to form an image. Both MIR and ECEI systems share large

collection optics for the reflected waves from the "cut-off layer" and vertically (poloidally) extended emission, respectively. Figure 2 illustrates a concept for a combined ECEI and MIR system employing refractive optics and a dichroic plate[11,12] (or an optimum beam splitter if the detection sensitivity is adequate) to separate the ECEI and MIR signals in frequency space. This configuration reflects MIR frequencies below *95 GHz* while transmitting the ECEI frequencies at *110 GHz* or above. Through experimental campaigns, it was found that a single beam splitter (electroformed metal mesh ~ 100 LPI) is suitable to provide the required S/N level for both systems. In this system, the primary components (poloidal and toroidal mirrors) of a microwave optical system are shared between the ECEI and MIR subsystems, with each subsystem using a dedicated high-resolution multichannel detector array based on the dual dipole antenna array which has significantly better antenna patterns and superior sensitivity compared with the previous generation detection arrays based on slot bow-tie antenna. A 3-D diagram of the TEXTOR combined system is shown in Fig. 3, including the TEXTOR tokamak, the primary focusing mirrors, and the two diagnostic subsystems.

In an imaging diagnostic, it is essential to make use of as large an acceptance aperture as possible. In the TEXTOR system, the limiting aperture occurs at the vacuum window, which is *42 cm* high, *30 cm* wide, located *57 cm* from the plasma boundary. All other optics have been adapted to make use of the full window aperture.

The primary difference between the configuration of the MIR and ECEI subsystems is that the MIR system has the added complication of the probing beam. In order to maximize the robustness of the collection optics to details of the plasma profile, the probing beam is focused at the center of the radius of curvature of the cutoff surface, so that the incident wavefront matches

the shape of the reflecting layer. The focal point is, of course, different in the poloidal and toroidal directions. The optics are designed so that both the illumination beam and reflected signal can be focused using the two fixed primary mirrors. A beam splitter separates the transmitted beam path from the detection path and final detector optics.

3. ELECTRON CYCLOTRON EMISSION IMAGING (ECEI)

Electron cyclotron emission measurements have been routinely used to measure profiles[13] and fluctuations of electron temperature of the plasmas such as sawteeth oscillations,[14,15] in magnetized toroidal plasmas since 1974. In a conventional ECE radiometer, a horn antenna receives the ECE radiation at the outboard side, which is separated into different frequency bands, each corresponding to a different horizontal location in the plasma as illustrated in Fig. 4a. A number of efforts have been directed toward techniques aimed at obtaining 2-D T_e profile measurements by ECE. In JET, several ECE radiometers were constructed and configured to measure the plasma along different angles.[16] Another way to project 2-D T_e profile relies on the assumption that the plasma rotates poloidally as a rigid body; therefore, the time variations measured by a 1-D ECE system near the plasma mid-plane can be interpreted as poloidal variation[14,15]. Important experimental results regarding plasma equilibrium[16] and MHD fluctuations[14,15] have been obtained using this approach.

In the ECE Imaging approach, the single antenna of a conventional heterodyne ECE radiometer is instead replaced by an array of antennas, using large diameter optics to image the plasma onto the array, which transforms the 1-D radiometer into a 2-D imaging diagnostic as shown in Fig. 4b. ECE radiation is collected and imaged onto a mixer/receiver array comprised

of planar antennas with integrated Schottky diodes. This arrangement has the advantages of wide radio frequency (RF) and intermediate frequency (IF) bandwidths, ease of fabrication, and low cost. The vertically arranged array elements are aligned along the **E** field (vertical) direction to collect second harmonic X-mode radiation. Large diameter optics image the plasma onto the array, enabling each array element to view a distinct plasma chord. Using the one-to-one mapping of ECE frequency to major radius in tokamak plasmas allows the ECEI focal plane to be swept through the plasma by sweeping the receiver frequency of the array, thereby forming 2-D images of the T_e profile.[17] Using the intermediate ECEI system, there was an extensive study of random fluctuation of electron temperatures[6,9].

The success of ECEI is due, in large part, to its ability to form high resolution T_e images. For the ECEI measurements performed thus far on tokamaks, the compact imaging array, the large horizontal port, as well as the large aperture imaging optics all contribute to achieve the superior spatial resolution of the ECEI system in the transverse direction of the sightlines.[18,19] The key is to match the desired Gaussian beam pattern in the plasma to the antenna reception angle. Horizontally, the sample volume size is limited by the RF bandwidth as well as the radiation bandwidth which arises from the magnetic field gradient, Doppler broadening, and relativistic broadening.[18,19] In the various ECEI systems developed to date, the characteristic sample volumes (1/e power) were ~1 cm in both the radial and poloidal directions.

Figure 5a illustrates the optical layout of the TEXTOR ECEI system and vertical extent of focal plane when it is aimed at a layer close to the q~1 surface ("inversion radius"). The position of the image plane with a similar vertical extent can be varied by adjusting the first lens close to the substrate lens for the detector array and an example for a field of view close to the q~3 surface is shown in Fig. 5b. As demonstrated, the vertical image height does not change

significantly across the entire plasma. Since most of the ECEI sightlines are off-axis, refraction effects become important at high densities. From ray-tracing calculations, it is found that the focusing effect of the plasma is not important, i.e. the beam waist location and spot size within the plasma are relatively unaffected, while the bending of the sightline can be quite significant.[20] This can be corrected in the data analysis with readily obtainable density profiles in most machines, since the sightlines in vacuum are accurately measured.

In the new ECEI system installed on TEXTOR, a multi-frequency heterodyne receiver is constructed for each of the imaging channels, so that 2-D maps of T_e profiles and fluctuations can be obtained in a single discharge. This new ECEI diagnostic represents a breakthrough in 2-D electron temperature profile and fluctuation measurements. For the study of $\tilde{T}_e$ turbulence, the instrument makes it possible to simultaneously and unambiguously measure $< k_r >$ and $< k_\theta >$ (time averaged), which is essential for mode identification. In the case of T_e profiles and coherent mode phenomena such as various MHD activity, this will allow direct observation of island/rotation without the assumption of rigid body rotation. The 2-D mapping also makes it considerably easier to overlap with MIR sample volumes for correlation studies between $\tilde{T}_e$ and $\tilde{n}_e$ fluctuations together with the imaging flexibility of the ECEI system as shown in Figs. 5(a) and 5(b).

The 20 channel dual dipole printed circuit antenna/mixer imaging array incorporating wideband baluns and low noise microwave preamplifiers was introduced for the new ECEI detection array for the first time[10]. Wide RF bandwidth has been achieved using a high power ELVA-1 90-136 GHz BWO as the Local Oscillator (LO) source. Owing to the improved sensitivity with dual dipole antenna elements, LO drive is sufficient for the 105-127 GHz tunable

bandwidth of the present system. The collected ECE radiation over a broad frequency range through the optical view is downconverted with a fixed frequency LO to provide a wide IF bandwidth input signal. Once amplified, the input signal is then divided into 8 equal parts using a printed divider designed on microstrip transmission line. The divided signals then mixed down, each with a distinct LO frequency (~500 MHz separation and ranging from ~3 GHz to ~7 GHz), using low cost balanced mixers. A total of 8 LO signals are needed to downconvert the 2-D ECEI signals, with 16 LO outputs per frequency. Each LO signal is generated from a low cost VCO, which is power divided and amplified using low cost, low noise gain blocks. The mixer outputs are bandpass filtered (5-150 MHz), rectified and amplified for acquisition and analysis.

The logical test T_e fluctuation measurement for the new ECEI system is m=1 oscillations (sawteeth), since the fluctuation level is large and the general physics of sawteeth phenomena is relatively well understood. The fundamental physical process of magnetic reconnection is still an outstanding issue, however, and requires 2-D measurement of T_e and plasma current to understand the entire reconnection process. Primary outstanding issues are; (1) whether the reconnection process is partial (localized in poloidal and toroidal space) or full, (2) whether the physics of the sawtooth crash is due to ballooning or kink modes. There has been significant effort devoted toward 2-D and 3-D reconstructions of the dynamics of sawteeth phenomena via X-ray tomography and fast ECE measurements. In X-ray tomography, an interpretation problem arising from multi-plasma parameters (density, temperature and impurity contents), reconstruction process based on line measurement has been a lingering issue. 3-D or 2-D reconstruction of 1-D ECE measurement is heavily dependent upon MHD modeling which requires many assumptions.

TEXTOR resumed operation in late 2003 after a major upgrade of the hardware, and most of the diagnostic systems are still in the "recovery" phase. The test plasma conditions for the ECEI experiment were as follows; I_p = 400 kA, B_t = 2.3-2.4 T, $n_e(0)$= 2- 4 10^{13}/cm^3, and $T_e(0)$ ~1 keV. Since the radial resolution is limited to ~6 cm near the core, radial extensions of the image can be obtained by varying either the toroidal field or the LO frequency on a shot-to-shot basis. Since the system is not currently absolutely calibrated, the measured voltage of each channel (proportional to the local electron temperature) is normalized to the average value and the ratio is multiplied to $T_e(r)$ profile measured by Thomson scattering. In order to reduce the noise level further, ~10 identical "sawteeth" oscillations are averaged. The sequence of "sawteeth" crash is clearly illustrated in Fig. 7. Note that inversion radius drawn here may not be an accurate quantity due to lack of current profile measurement (q~1). Here, the hot island approaches the inversion radius and reconnects to the magnetic surface of the inversion radius at the low field side without high poloidal number ballooning mode. After the reconnection process is completed, heat spreads in the mixing zone along the inversion radius while the cold island sets in inside of the inversion radius. Here, the crash time is ~150 μsec and one period of m=1 mode is ~170 msec. The reconnection process shown here is similar to the "x-point like" magnetic reconnection and supports the concept of local reconnection (poloidally and toroidally) theory in the lower field side without ballooning characteristics. In order to visualize the heat transfer out of the inversion radius to the mixing zone, a sequence of the heat transfer processes is illustrated in Fig. 8 by a composition of three images obtained from three discharges with slightly different magnetic field (2.3T, 2.35T and 2.4T). The preliminary analysis demonstrates that the temperature in the vicinity of the inversion radius is not perturbed through the crash whereas the hot spot is clearly present before and after the crash. This observation indicates that the

ballooning characteristic is absent in these images. An alternative explanation may have to do with "x-point reconnection" which may be slightly different due to the variation of magnetic fields. A detailed understanding of the m=1 mode oscillation will be our immediate goal as soon as the core current profile measurement is available together with other important diagnostic information on TEXTOR. While a detailed physics study of m=1 mode reconnection process is in progress, the current ECEI system with a relatively small image but with high spatial resolution is ideal for the study of smaller magnetic island structures such as Neoclassical Tearing modes (NTM) and Double tearing mode which are harmful MHD phenomena for plasma stability near the q~2 surface.

In previous ECEI systems, the LO frequency was varied to accommodate experimental measurment, which gives rise to difficulties in system sensitivity calibration. This is important for temperature profile measurements, and a number of different methods were applied.[21] However, since the relative temperature fluctuation measurements do not depend on the sensitivity, the difficulty of calibration does not affect the application of ECEI in measuring the frequency and wavenumber spectra, as well as the relative fluctuation amplitude of T_e fluctuations. In the new ECEI system for TEXTOR, a fixed frequency LO source is utilized, so that the sensitivity can be conveniently calibrated using the standard hot-cold load technique as employed for conventional radiometers. This independently calibrated ECEI system may be applicable to the study of plasmas with non-Maxwellian electron distribution functions.[18,19]

3. MICROWAVE IMAGING REFLECTOMETRY (MIR)

In contrast to the ECEI system, the MIR system is more complex and sophisticated, as noted in the previous section. Prior to the commissioning of the MIR system on TEXTOR, an

extensive laboratory testing was performed[7,8], verifying the system optical performance. Through several experimental campaigns on TEXTOR, many tests were performed to ensure that the performance of the system satisfied the design specifications.

A time history of one of the central MIR channels is illustrated in Fig.8, together with the plasma density profile evolution which is closely tied to the motion of the cut-off layer. For the earlier part of the discharges, the quadrature signal has well defined phase information with relatively small amplitude modulations. As the plasma density is increased, the level of amplitude modulation is increased as indicated in the quadrature signal. Except for one non-working channel (due to a bad diode), all 15 channels revealed similar characteristics.

Using the measured spectra from the MIR system, a preliminary spectral analysis was performed, as shown in Fig. 9. The magnitude of the cross-coherency of the complex quadrature signals is presented in Figs. 9a-9c, for channels spaced 0.6, 5.0, and 9.4 cm from the reference channel, respectively. The cross-coherency also yields a phase lag between each spectral component for each spatially separated channel pair. The magnitude of the cross-coherency, plotted against both the frequency and the phase lag divided by the channel spacing (summed for all channel pairs), is presented as a surface plot in Fig. 9d. The slope of this plot yields the poloidal velocity of the turbulent structures over a wide spectral range, and is weighted by the channel pairs exhibiting the highest coherency. This type of plot is also presented in Figs. 10c and 10d, for two timeslices taken during neutral-beam injection heating and just after the turnoff of the neutral beam, respectively. The corresponding complex spectra for a central channel are shown in Figs. 10a and 10b. During the NBI injection, the frequency spectrum is broad and the derived rotation speed is +21 km/sec, corresponding to the ion diamagnetic direction. Once the

heating beam is turned off, the plasma slows down within a beam slowing down scale and settles at -12 km/sec in the electron diamagnetic direction.

SUMMARY

Using the significant advances in millimeter wave imaging technology, a microwave imaging system for simultaneously measuring electron density and temperature fluctuations has been applied to TEXTOR plasmas. A true 2-D image of electron temperature covering an m=1 oscillation were captured by the 128 channel ECEI system thereby permitting the detailed study of the physics of magnetic reconnection phenomena on a fast time scale. Spectral analysis of the multichannel MIR data has yielded poloidally resolved spectra and assessments of poloidal phase velocity of turbulent structures. It is envisioned that 2-D images of both n_e and T_e fluctuations will be captured and compared with the images from theoretical computations in the future. In the coming years, such imaging techniques will be essential for the study of fluctuation physics in plasmas.

ACKNOWLEDGMENTS

This work is supported by the U.S. Department of Energy under contract Nos. DE-AC02-76-CH0-3073, DE-FG03-95ER-54295 and W-7405-ENG-48, by NWO and EURATOM. Thanks go to TEXTOR team for the various assistance and plasma operations.

REFERENCES

1. Z. Lin et al., Science **281**, pp. 1835-1837, (1998).

2. J. Candy, H.L. Berk, B.N. Breizman and F. Porcelli, *Nonlinear Modeling of Kinetic Plasma*

Instabilities, Phys. Plasmas **6** (1999) 1822.

3. W. Park, et al., Fusion Energy 1996 (Proc. 16th Int. Conf. Montreal, 1996), Vol. 2 IAEA, Vienna (1997) 411.

4. H. Park, et al., Rev. Sci. Instrum. **74**, pp. 4239-4262, (2003).

5. E. Mazzucato, Nuclear Fusion **41**, pp. 203-213, (2001).

6. B. H. Deng, D. L. Brower, G. Cima, C. W. Domier, N. C. Luhmann, and C. Watts, Phys. Plasmas **5**, pp. 4117-4120, (1998).

7. T. Munsat, E. Mazzucato, H. Park, et al., Rev. Sci. Instrum., **74**, 0000, (2003)

8. T. Munsat, E. Mazzucato, H. Park, C.W. Domier, N. C. Luhmann, Jr., A J H Donne, M. van de Pol., Plasma. Phys. & contl. Fusion. **45,** 469-487, (2003).

9. G. Cima, et al., Fusion Energy and Design, 34-35, (7th International Toki Conference on Plasma Physics and Controlled Nuclear Fusion, Toki, Japan, Nov. 28-Dec. 1, 1996) pp. 515-518, (1997).

10. C.W. Domier et al., at this conference

11. P. Siegel, R. R. J. Dengler, J. C. Chen, IEEE Microwave and Guided Wave Letter, 1, pp 8, (1991)

12. H. H. Javadi, and P. H. Siegel, JPL New Technology Report NPO-20826, pp 1-8, (2001)

13. G. Taylor, et al., Rev. Sci. Instrum. **56**, 928 (1985)

14. E. Westerhof, P. Smeulders, N. Lopez Cardozo, Nuclear fusion, **29**, no. 6 (1989) 1056-1061.

15. Y. Nagayama, et al., Phys. Plasmas, **3**, 1647 (1996).

16. D. V. Bartlett, D. J. Campbell, A. E. Costley, et al, Proc. 14th European Conference on Controlled Fusion and Plasma Physics, **11D**, part III, pp 1252-1255, Madrid (1987)

17. B. H. Deng, S. R. Burns, C. W. Domier, T. R.Hillyer, R. P.Hsia, N. C. Luhmann Jr., D. L. Brower, G. Cima, A. J. H. Donné, T. Oyevaar, RTP team, Fusion Engineering and Design **53**, pp.77-85, (2001).

18. V. Krivenski, Fus. Eng. and Design, **53**, pp. 23-33 (2001))

19. E.de la Luna, et al, Rev. Sci. Instrum. **19**, pp. 193, (2003)

20. R. P. Hsia, B. H. Deng, W. R. Geck, C. Liang, C. W. Domier, and N. C. Luhmann, Jr., Rev. Sci. Instrum. **68**, pp. 488, (1997).

21. B. H. Deng, et al., Phys. Plasmas **8**, no. 5, pp. 2163-2169, (2001).

FIGURE CAPTIONS

Fig.1. Characteristic frequencies for the TEXTOR plasma.

Fig. 2. Concept of a simultaneous microwave imaging system for density and temperature fluctuation measurement.

Fig. 3. 3-D CAD picture of the engineering design of the TEXTOR ECEI/MIR system

Fig. 4. (a) Conventional ECE system utilizes a single detector and wideband sweeping local oscillator source. (b) ECEI system with a quasi-optical 1-D detector array. It is similar to the many vertical layers of a conventional ECE system.

Fig. 5. Ray tracing of ECEI imaging plane located near the q~1 surface (a). The field of view can be moved to the q~3 surface by adjusting a lens close to the detection system as shown in (b)

Fig. 6. Eight frames of the m=1 mode during the crash phase. The “hot island” approaches the

inversion radius before the crash at the lower field side of the magnetic configuration. Heat spreads along the inversion radius and the cold island develops and sets in inside the inversion radius. The process is indicative of "x-point" magnetic reconnection in the partial reconnection model. Note that the double white lines represent the estimated inversion radius.

Fig, 7. Six frames of the crash process, emphasizing heat transfer out of the inversion radius are illustrated through a composition of the three 2-D images (384 pixels) obtained by varying the toroidal magnetic fields (2.3T, 2.35T and 2.4T). Note that the double white lines are an estimated inversion radius.

Fig. 8. Time history of one of the central MIR detectors with 2-D plasma density. The level of amplitude modulation is significantly increased as the density is increased. The quadrature signal indicates less amplitude modulation in the low density region.

Fig. 9. Cross-coherency as a function of frequency for channel #10. (a) vs. #9 (0.66 cm) (b) vs. #5 (5.0 cm) (c) vs. #1 (9.4 cm). (d) Average cross-coherency value of frequency bin for #10 with respect to the separation distance of the imaging spots for all channels.

Fig. 10. Poloidal velocity of turbulent spectra. NBI is turned off at 4.5 sec. (a) Broad frequency spectra and estimated initial velocity is +21 km/sec during NBI (co-beam) (4.4 sec) (b) Narrow frequency spectra after NBI off. Rotation reverses and settles at -12 km/sec (4.8 sec)

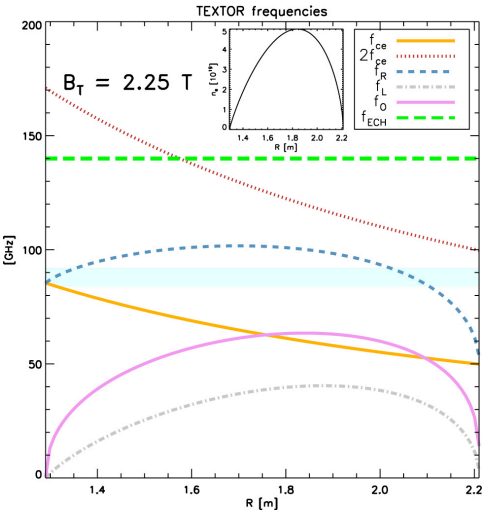

FIG. 1

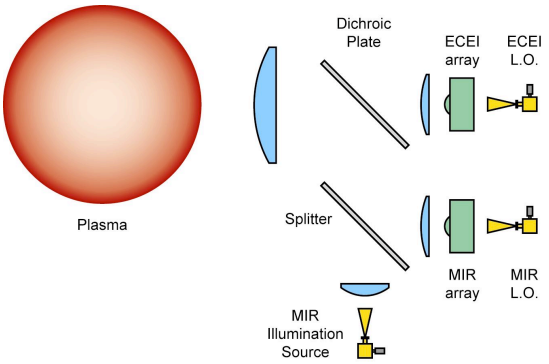

FIG.2

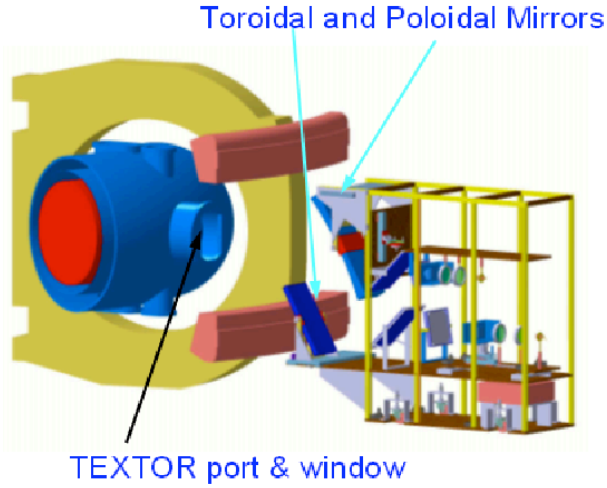

FIG.3

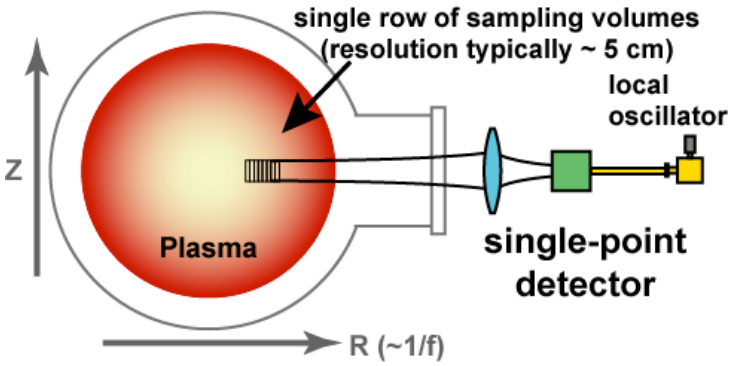

FIG.4a

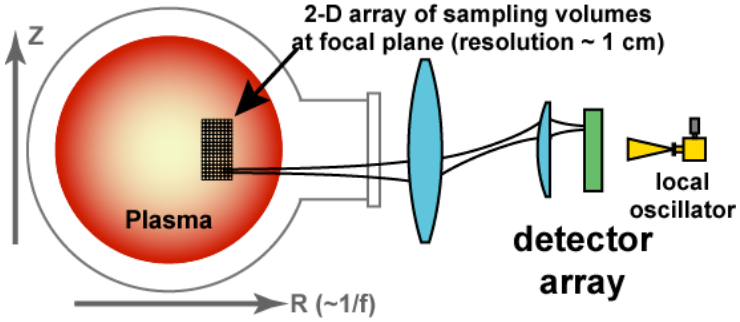

Fig. 4b.

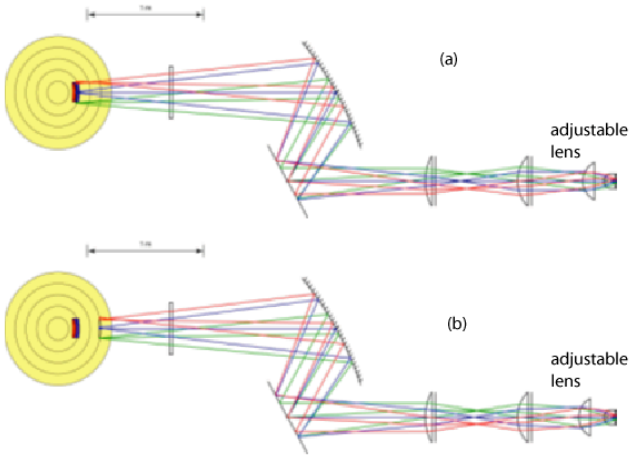

FIG.5

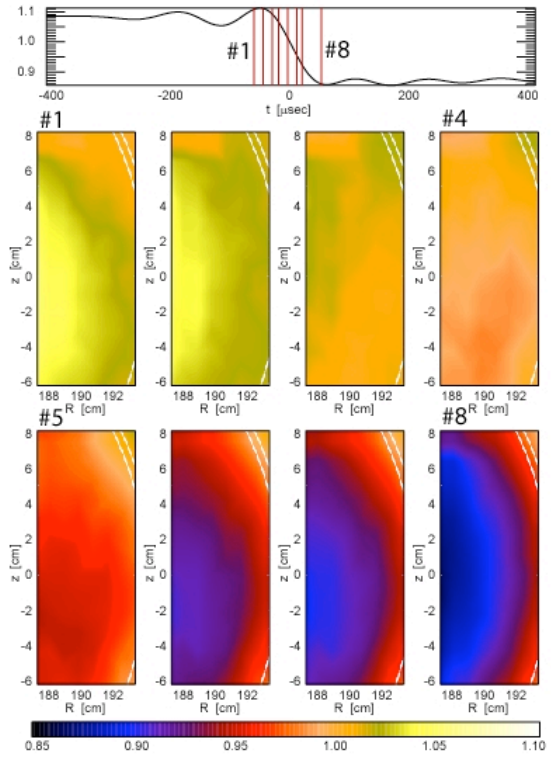
#1
#8
t [μsec]
#1
#4
#5
#8
z [cm]
R [cm]
0.85 0.90 0.95 1.00 1.05 1.10

Fig. 6

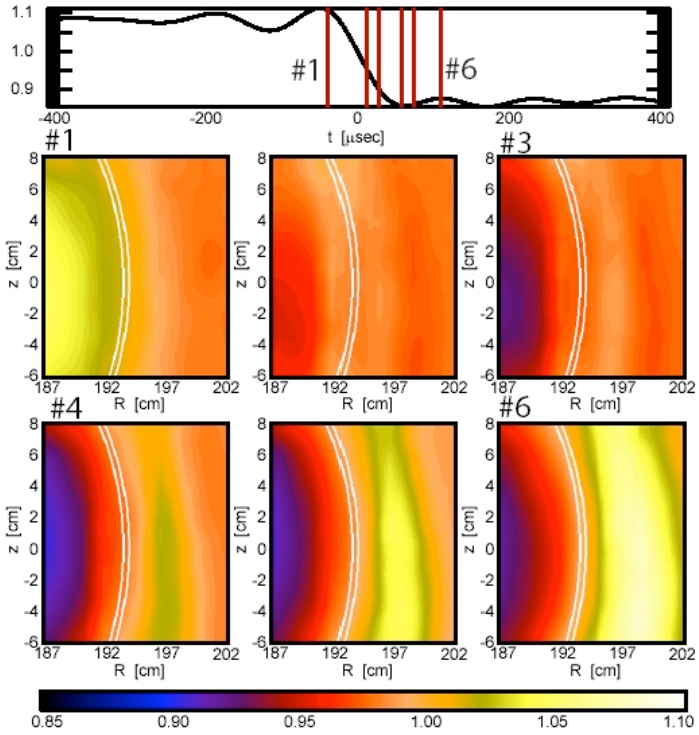
#1
#6
t [μsec]
#1
#3
#4
#6
z [cm]
R [cm]
0.85 0.90 0.95 1.00 1.05 1.10

Fig.7

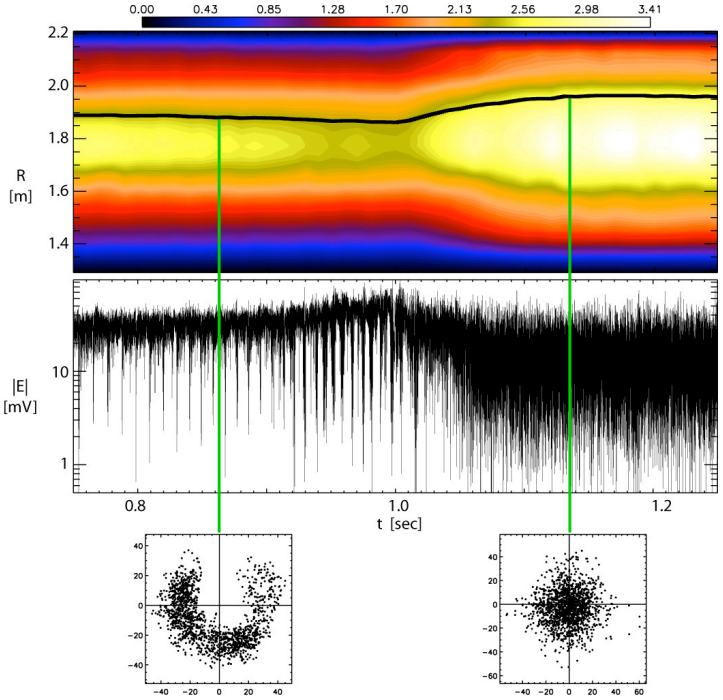
0.00
0.43
0.85
1.28
1.70
2.13
2.56
2.98
3.41
R
[m]
|E|
[mV]
t [sec]

Fig. 8

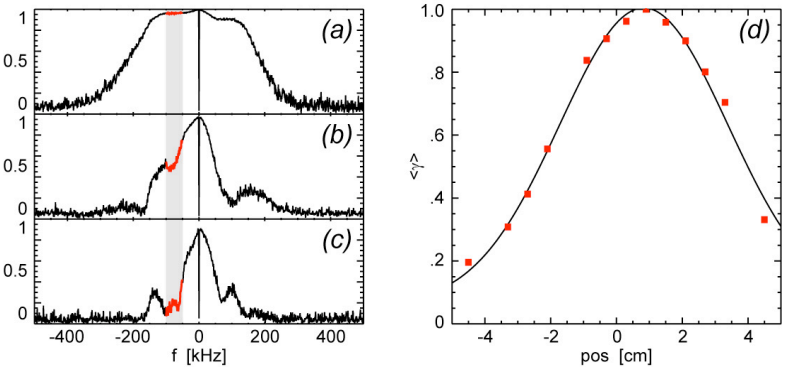
(a)
(b)
(c)
(d)
f [kHz]
pos [cm]
<γ²>

Fig. 9

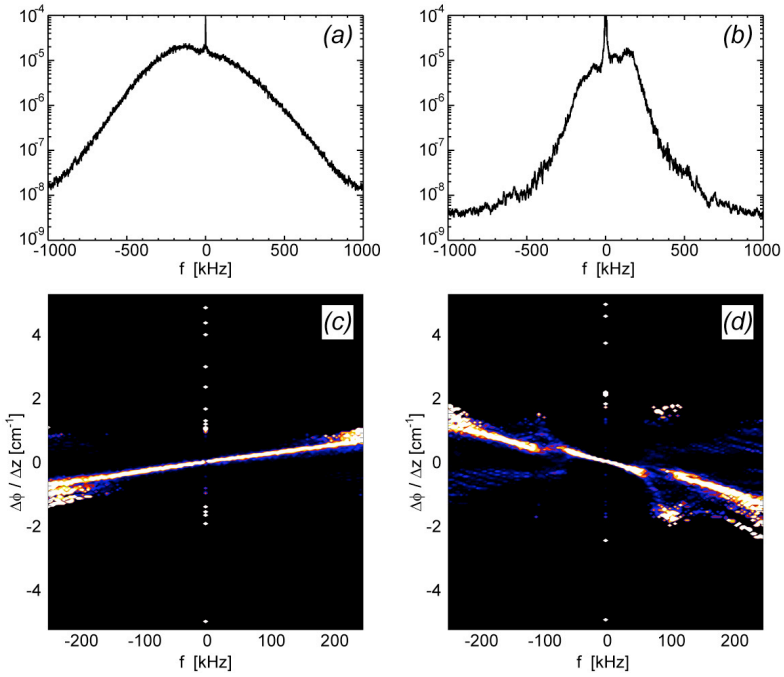

Fig. 10

External Distribution

Plasma Research Laboratory, Australian National University, Australia

Professor I.R. Jones, Flinders University, Australia

Professor João Canalle, Instituto de Fisica DEQ/IF - UERJ, Brazil

Mr. Gerson O. Ludwig, Instituto Nacional de Pesquisas, Brazil

Dr. P.H. Sakanaka, Instituto Fisica, Brazil

The Librarian, Culham Laboratory, England

Mrs. S.A. Hutchinson, JET Library, England

Professor M.N. Bussac, Ecole Polytechnique, France

Librarian, Max-Planck-Institut für Plasmaphysik, Germany

Jolan Moldvai, Reports Library, Hungarian Academy of Sciences, Central Research Institute for Physics, Hungary

Dr. P. Kaw, Institute for Plasma Research, India

Ms. P.J. Pathak, Librarian, Institute for Plasma Research, India

Ms. Clelia De Palo, Associazione EURATOM-ENEA, Italy

Dr. G. Grosso, Instituto di Fisica del Plasma, Italy

Librarian, Naka Fusion Research Establishment, JAERI, Japan

Library, Laboratory for Complex Energy Processes, Institute for Advanced Study, Kyoto University, Japan

Research Information Center, National Institute for Fusion Science, Japan

Dr. O. Mitarai, Kyushu Tokai University, Japan

Dr. Jiangang Li, Institute of Plasma Physics, Chinese Academy of Sciences, People's Republic of China

Professor Yuping Huo, School of Physical Science and Technology, People's Republic of China

Library, Academia Sinica, Institute of Plasma Physics, People's Republic of China

Librarian, Institute of Physics, Chinese Academy of Sciences, People's Republic of China

Dr. S. Mirnov, TRINITI, Troitsk, Russian Federation, Russia

Dr. V.S. Strelkov, Kurchatov Institute, Russian Federation, Russia

Professor Peter Lukac, Katedra Fyziky Plazmy MFF UK, Mlynska dolina F-2, Komenskeho Univerzita, SK-842 15 Bratislava, Slovakia

Dr. G.S. Lee, Korea Basic Science Institute, South Korea

Institute for Plasma Research, University of Maryland, USA

Librarian, Fusion Energy Division, Oak Ridge National Laboratory, USA

Librarian, Institute of Fusion Studies, University of Texas, USA

Librarian, Magnetic Fusion Program, Lawrence Livermore National Laboratory, USA

Library, General Atomics, USA

Plasma Physics Group, Fusion Energy Research Program, University of California at San Diego, USA

Plasma Physics Library, Columbia University, USA

Alkesh Punjabi, Center for Fusion Research and Training, Hampton University, USA

Dr. W.M. Stacey, Fusion Research Center, Georgia Institute of Technology, USA

Dr. John Willis, U.S. Department of Energy, Office of Fusion Energy Sciences, USA

Mr. Paul H. Wright, Indianapolis, Indiana, USA

The Princeton Plasma Physics Laboratory is operated
by Princeton University under contract
with the U.S. Department of Energy.

Information Services
Princeton Plasma Physics Laboratory
P.O. Box 451
Princeton, NJ 08543

Phone: 609-243-2750
Fax: 609-243-2751
e-mail: pppl_info@pppl.gov
Internet Address: http://www.pppl.gov